Experimental Study of Volatile Products Generated by Ring-Opening Reactions during Syringol Pyrolysis

Jianli Huang, Huamei Yang *

School of Materials and Chemical Engineering, Xuzhou University of Technology, Xuzhou, Jiangsu 221018, China

* Corresponding Author: Huamei Yang

Abstract

Ring-opening reactions to support the formation of CO, CO_2 and C_1-C_5 light hydrocarbons (C_1-C_5 LHs) is one important pathway in vapor-phase reactions during lignin pyrolysis. Syringyl structure is rich in primary volatile products generated from lignin pyrolysis, and inevitably involved in vapor-phase reactions. However, there is less available information to elucidate the mechanism of syringol pyrolysis. In this work, syringol was pyrolyzed in a tubular reactor at 550-950 °C (0.5s) and at 750 °C(0.1-4.2 s). Distributions of volatile products from syringol pyrolysis were quantified by online GCs, focused on CO, CO_2, C_1-C_5 LHs, phenols, light oxygenated compounds and aromatic products. Syringol was decomposed dramatically above 750 °C with residence time 0.5 s. Main volatile products were CO, CO_2 and C_1-C_5 LHs, which were possibly formed by ring-opening reactions of syringol. C_1-C_5 LHs were consumed to support the formation of aromatic hydrocarbons. Detailed data were provided in this communication, and is significant to theoretically investigate the process of syringol pyrolysis with the aim to elucidate the pyrolysis mechanism of syringyl structure during lignin pyrolysis.

Keywords

Syringol; Pyrolysis; Ring-opening Reaction; Inorganic Gases; C_1-C_5 Hydrocarbons.

1. Introduction

Pyrolysis of lignin has been studied extensively because of its potential to provide electric power, and/or to produce renewable carbon-based fuels and valuable chemicals.[1-2] Understanding the mechanism of lignin pyrolysis is of great importance for improvement of thermochemical conversion processes and upgrading of biofuel.[1, 3] Worldwide efforts are being made to experimentally and numerically investigate the products distribution and reaction pathways during lignin pyrolysis.[4-6] However, it is still a tough task to elucidate the pyrolysis mechanism comprehensively since pyrolysis behaviors and products distribution are varied with pyrolysis conditions (temperature, pressure, heating rate, residence time, etc.) [5-10] and composition ratio of guaiacyl (G), syringyl (S) and p-hydroxylphenyl (H) units in lignin.[11-12] Lignin model compounds provide us chances to clarify the pyrolysis mechanism of lignin. Pyrolysis of dipolymers or oligomers were experimentally or numerically investigated to understand the breakage of carbon-oxygen ether bonds or carbon-carbon linkages among aromatic structures during the primary decomposition of lignin. [13-17] More than 50 wt% lignin was converted into volatiles at temperatures higher than 500 °C.[9] Volatiles escape from particles and continue to crack, combine, or condense in vapor phase. The vapor-phase reaction of volatiles is unavoidable during lignin pyrolysis.[5] Derivatives of phenol, guaiacol, and syringol are main volatile compounds generated from lignin pyrolysis.[9] Their decomposition was involved in vapor-phase reactions and decides the final products distribution. Recently, monomer model compounds (Phenol, anisol, benzenediol, eugenol, vanillin, etc) have been experimentally or numerically studied to investigate the vapor-phase reactions during lignin pyrolysis. [18-24] The ring-opening reactions of aromatic structure were elucidated for the formation of inorganic gases and light hydrocarbons in vapor-phase reactions.

Syringyl together with guaiacyl and p-hydroxylphenyl are three main structures in lignin, resulting in large amount of syringol and its derivatives generated from lignin pyrolysis.[9-10] Syringol and its derivatives are rich in volatile as primary products, and inevitably involved in vapor-phase reactions. However, there is less available information on the products distribution (especially inorganic gases and C_1-C_5 light hydrocarbons), [25, 26] which limits us to elucidate the pyrolysis mechanism of syringyl structure during lignin pyrolysis. With the purpose to elucidate the mechanism of syringol, this communication provides quantitative products information of syringol pyrolysis at 550-950 ^{o}C with residence time 0.1-4.2 s, which is important and significant for the mechanism elucidation and process simulation of syringol or lignin pyrolysis in the future work.

2. Results and Discussion

Syringyl structure is rich in primary volatile products generated from lignin pyrolysis, and decomposed in vapor-phase reactions. To elucidate the pyrolysis mechanism of syringol and clarify the vapor-phase reactions during lignin pyrolysis, this work provided essential information about syringol pyrolysis at 550-950 ^{o}C (0.5 s) and at 750 ^{o}C(0.1-4.2 s). All the products were clarified into five groups as inorganic gases (IGs), light hydrocarbons (LHs), light oxygenated compounds (LOCs), aromatic hydrocarbons (AHs) and phenols (PHOs). Differences between conversion rate and total yields of detected products were caused by the formation of products with heavy-molecular weight such as tar and soot, which were named as undetected products (UDCs) in this paper. Conversion rate and the distribution of products were presented in **Figure 1** and **Figure 2**.

2.1. Effect of Temperature

2.1.1. Conversion Rate and UDCs

Conversion rate of syringol increased quickly from 32.48 wt% to 94.74 wt% with temperature increasing from 550 ^{o}C to 750 ^{o}C, and syringol was completely decomposed above 750 ^{o}C as shown in **Figure 1(a)**. Components of UDCs would be very different at temperature below 750 ^{o}C and above 750 ^{o}C. Yield of UDCs increased from 19.46 wt% at 550 ^{o}C to 43.77 wt% at 650 ^{o}C, and then reduced to 27.59 wt% at 750 ^{o}C. Above 750 ^{o}C, yield of UDCs increased to 41.32 wt% at 950 ^{o}C. Large amount of coke was observed on the reactor-wall during syringol pyrolysis above 750 ^{o}C, which lead to the increasing high yield of UDCs above 750 ^{o}C. It was noted that no coke was observed at 550 ^{o}C and 650 ^{o}C. Components of UDCs would be some oxygenated intermediates from syringol decomposition. Those oxygenated intermediates were quickly decomposed to support the formation of IGs and LHs at 750 ^{o}C, leading to the obviously increasing yield of IGs and LHs at 750 ^{o}C as shown in **Figure 1(a)**.

2.1.2. Inorganic Gases (IGs).

IGs is one of main product groups, including CO, CO_2 and H_2 from syringol pyrolysis. There was less IGs generated at low temperature with its total yield being 0.01wt% at 550 ^{o}C and 1.52 wt% at 650 ^{o}C. Total yield of IGs increased dramatically to 31.79 wt% at 750 ^{o}C, and then slightly increased to 37.52 wt% with temperature increasing to 950 ^{o}C. The main components in IGs are CO and CO_2, and yields of CO and CO_2 are shown in **Figure 1(b)**. Yields of CO increased dramatically from 1.3 wt% at 650 ^{o}C to 22.57 wt% at 750 ^{o}C, and then slightly increased to 27.44 wt% with temperature increasing to 950 ^{o}C. Yield of CO_2 exhibited a similar trend with yield of CO, but CO_2 had a much lower yield than CO, being 9.10 wt% at 750 ^{o}C and 9.55 wt% at 950 ^{o}C.

2.1.3. C_1-C_5 light hydrocarbons (C_1-C_5 LHs).

Total yield of C_1-C_5 LHs increased from 4.4 wt% at 550 °C to 19.38 wt% at 750 °C, and then reduced to 11.88 wt% at 950 °C as shown in **Figure 1(a)**. Yields of C_1-C_5 LHs are shown in **Figure 1(c)**. Methane and C_2 LHs were easily formed by the combination of CH_3 with H or CH_3, and had much higher yields than C_3-C_5 LHs. Yield of methane monotonically increased from 1.05 wt% to 8.13 wt% with temperature increasing from 550 °C to 950 °C. Yield of C_2 LHs got its maximum (8.52 wt%) at 750 °C, and then reduced to 2.29 wt% at 950 °C. C_3-C_5 LHs exhibited similar trends with C_2 LHs, and got their maximum (2.09 wt%, 1.28 wt%, and 2.23 wt% respectively) at 750 °C, and then reduced with temperature increasing to 950 °C.

2.1.4. Light Oxygenated Compounds (LOCs).

The detected LOCs in this study were mainly methanol, acetaldehyde and acraldehyde as shown in **Figure 1(d)**. Methanol could be formed by the combination of OCH_3+H radical, or CH_3+OH, and was detected at temperature as low as 550 °C with its yield being 1.06 wt%. Mathanol got its maximum (4.14 wt%) at 750 °C, and completely consumed above 750 °C. Yields of acetaldehyde and acraldehyde were much lower than methanol. Acraldehyde has been detected at temperature as low as 550 °C, and achieves its maximum at 750 °C. Then Acraldehyde was decomposed to C_2 LHs and CO above 750 °C. Acetaldehyde has been detected at 550 °C with its yield being 0.52 wt% from syringol decomposition, and its yield reduces with temperature increasing.

2.1.5. Phenols (PHLs) and Aromatic Hydrocarbons (AHs).

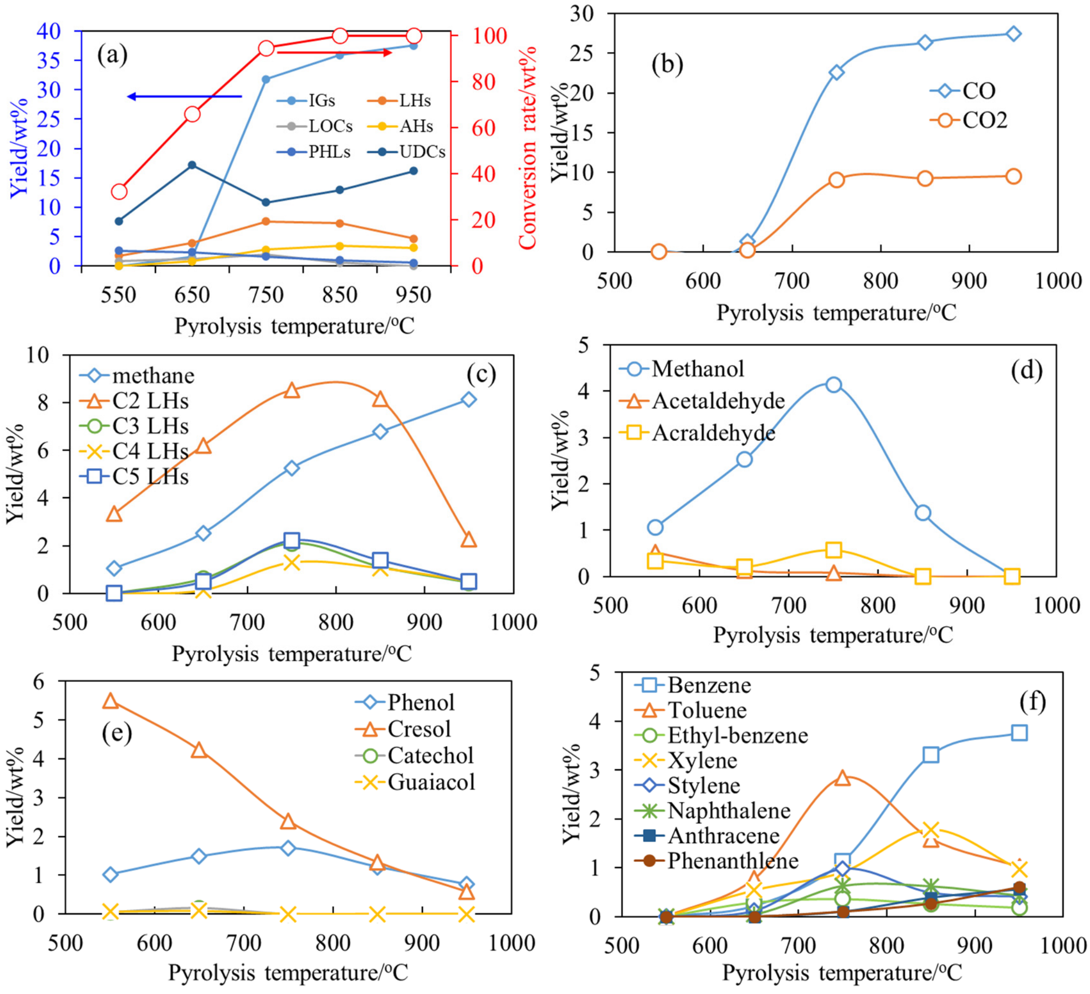

Figure 1. Conversion rate and products distribution from syringol pyrolysis at 550-950 °C, 0.5 s.

Yield of PHLs reduced from 6.64wt% at 550 ^{o}C to 1.34wt% at 950 ^{o}C as shown in **Figure 1(a)**. PHLs detected from syringol pyrolysis were mainly phenol and cresol as shown in **Figure 1(e)**. Yield of cresol reduced monotonically from 5.51 wt% to 0.58 wt% with temperature increasing from 550 ^{o}C to 950 ^{o}C. Yield of phenol got its maximum (1.70 wt%) at 750 ^{o}C, and then reduced to 0.76 wt% at 950 ^{o}C. Guaiacol and catechol were also detected with a much lower yield, lower than 0.15 wt%. Yields of AHs increased from 0 wt% at 550 oC to 8.71 wt% at 850 ^{o}C, and then reduced to 7.94 wt% at 950 ^{o}C as shown in **Figure 1(a)**. AHs mainly included benzene, toluene, styrene, ethyl-benzene, xylene, naphthalene, anthracene, and phenanthlene, and their yields were illustrated in **Figure 1(f)**. Yield of benzene increased from 0.22wt% to 3.76wt% with temperature increasing from 650 ^{o}C to 950 ^{o}C. Toluene got its maximum yield (2.85 wt%) at 750 ^{o}C, and reduced to 1.02 wt% at 950 ^{o}C. Styrene got its maximum yield (0.98 wt%) at 750 ^{o}C, and reduced to 0.41 wt% at 950 ^{o}C. Xylene got its maximum yield (1.78 wt%) at 850 ^{o}C, and reduced to 0.97 wt% at 950 ^{o}C. Yields of naphthalene, anthracene, and phenanthlene increased with temperature increasing to 950 ^{o}C, and their maximum yield were all lower than 0.70 wt%.

2.2. Effect of Residence Time

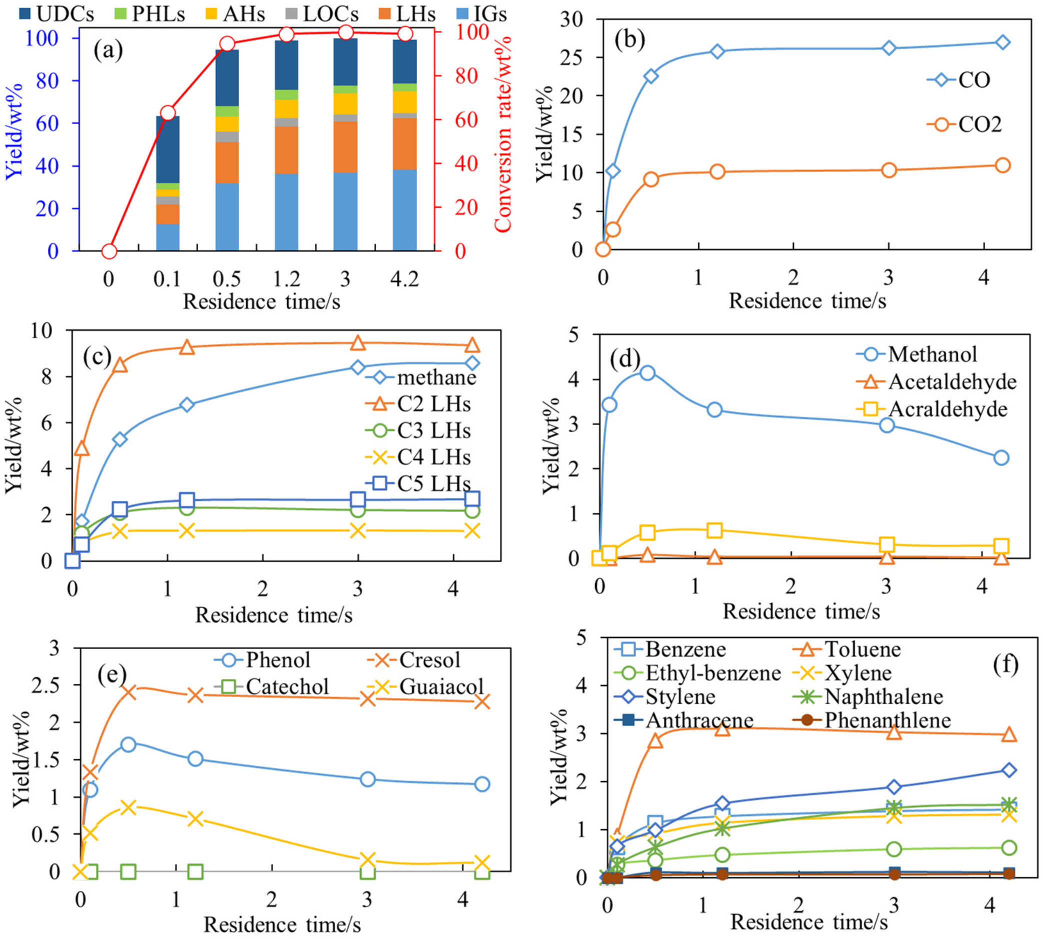

Figure 2. Conversion rate and products distribution from syringol pyrolysis at 750 ^{o}C, 0.1-4.2 s.

Syringol was significantly converted to IGs and C_1-C_5 LHs at 750 ^{o}C, indicating that the ring-opening reactions during syringol pyrolysis happened dramatically at 750 ^{o}C. The conversion rate and the distribution of products at 750 ^{o}C, 0.1-4.2 s were presented in **Figure 2**. Conversion rate of syringol was increased quickly at the first 0.5 s, and syringol was completely converted after 0.5 s as shown in **Figure 2(a)**. IGs, C_1-C_5 LHs and AHs were main detected products, and their yields were increased with residence time as shown in **Figure 2(a)**. Yields of all the detected products were quickly increased at the first 0.5 s as shown in **Figure 2(b)-(f)**. Yields of CO and CO_2 quickly increased to 25.82 wt% and 10.11 wt% at the first 1.2 s as shown in **Figure 2(b)**, and then slightly increased to 27.01 wt% and 11.00 wt% after 1.2 s, respectively. Methane and C2 LHs had a much higher yield than C_3-C_5 LHs. Yield of methane was monotonously increased with residence time to 8.59 wt%, while yields of C_2 LHs, C_4 LHs and C_5 LHs increased at the first 0.5 s as shown in **Figure 2(c)**, and then were kept stable or slightly increased after 0.5 s. Yield of C_3 LHs slightly reduced with residence time after 1.2 s as shown in **Figure 2(c)**. Yields of LOCs and PHLs got their maximum value at 0.5 s, and then reduced after 0.5 s as shown in **Figure 2(a), (d)** and **(e)**. Toluene had the highest yield in AHs. Yield of toluene got its maximum value (3.11 wt%) at 1.2 s, and then slightly reduced with residence time as shown in **Figure 2(f)**. Yields of benzene, styrene, ethyl-benzene, xylene, naphthalene, anthracene, and phenanthlene all increased with residence time.

3. Conclusion

With the purpose to investigate ring-opening reactions and to provide essential experiment information on syringol pyrolysis, thirty-six products generated from syringol pyrolysis at 550-950 °C, 0.5 s and at 750 °C, 0.1-4.2 s were quantified by online GCs, including IGs, C_1-C_5 LHs, AHs, LOCs, and phenols. Conversion rate of syringol increased remarbly at 750 °C with obviously increasing yields of IGs and LHs at 750 °C, indicating that ring-opening reactions happened dramatically above 750 °C to support the formation of IGs and LHs at 750 °C. Yield of CO and CO_2 increased with temperature and residence time. Maximum yield of CO was achieved at 27.44 wt%, while yield of CO_2 was much lower than yield of CO, and maximum yield of CO_2 was 11.00 wt%. The formation of methane was enhanced by increasing temperature and residence time with its maximum yield as 8.59 wt%. C_2-C_5 LHs achieved its maximum at 750 °C or 850 °C, and then consumed to support the formation of AHs with temperature increasing to 950 °C. Detailed data were provided in this communication, which is significant to theoretically investigate the process of syringol pyrolysis with the aim to elucidate the pyrolysis mechanism of syringyl structure during lignin pyrolysis.

4. Experimental Section

Syringol was purchased from Sigma-Aldrich Inc., USA (purity ≥ 99%), and was pyrolyzed in the presence of inert gas (Helium, He) at 241 kPa in a tubular reactor system with an online GC. The reactor system consists of a vaporizer, a quartz tubular-flow reactor and an online GC. First, the GC baseline was stabled by helium, and the tubular reactor is heated to expected temperature (550-950 °C) by a multi-stage furnace. Experiments were carried out by loading 1-mg sample into a Pyrex tube fixed in the vaporizer which is heated to 300 °C by an electric furnace, for vaporization of syringol. After around 10 min, vaporizer and tubular reactor were connected, and the sample vapor was pushed into the tubular reactor by helium. The quartz tubular-flow reactor was used for the decomposition of the sample, and its inner diameters of the tubular-flow reactor was 4 mm. Residence time can be controlled by the heated length of reactor inserted into the multi-stage furnace. All products were introduced into the online GC equipped with TCD and/or FID with carrier gas (helium) with a flow rate of 76 cm^3 min^{-1} (stp of 298.15 K, and 101.35 kPa). This work was focused on the ring-opening reactions during syringol pyrolysis, hence, the effort to detect the heavy-weight molecules was not included here. The chromatographic conditions and typical GC chromatograms along with the assigned peaks were set up to measure volatile products especially inorganic gases and C_1-C_5 hydrocarbons as our previous publications[5,19]. Products yield can be calculated by Equations (1) - (4) below. Each test was run three times, and the mean yields of detected products were employed to trend the products distribution with pyrolysis temperature at 550-950 °C and with residence time being

0.1-4.2 s. The repeatability examinations for the analytical pyrolysis experiments revealed that the relative errors of the product yield generally within ±10%.

Mass of product *i*,

standard substances are available:

$$m_i=\frac{A_i}{\left(\frac{A_{i\text{-st}}}{N_{i\text{-st}}}\right)}*M_i. \quad \text{Equation} \qquad (1)$$

standard substances are unavailable:

$$m_i=\frac{A_i}{\left(\frac{A_{\mathrm{CH_4}}}{N_{\mathrm{CH_4}}}\right)*R}*M_i. \quad \text{Equation} \qquad (2)$$

Yield of product *i*,

$$y_i=\frac{m_i}{m_{i\text{-feed}}}*100\%. \quad \text{Equation} \qquad (3)$$

Yield of UDCs

$$y_{\mathrm{UDCs}}=100\%-\sum y_i \quad \text{Equation} \qquad (4)$$

In these equations, m_i denotes the mass of product *i*; $m_{i\text{-feed}}$ denotes the mass of feed guaiacol; A_i denotes the peak area of product *i*; $A_{i\text{-st}}$ denotes the peak area of standard substances *i*; $N_{i\text{-st}}$ denotes the moles number of standard substances *i*; M_i denotes the mass weight of product *i*; R_i denotes the response factor of effective carbon number; y_i denotes the yield of product *i*.

References

[1] Chen, W. H., Farooq, W., Shahbaz, M., Naqvi, S. R., Ali, I., Al-Ansari, T., and Amin, N. A. S., *Energy*, 2021, 226, 120433.

[2] Pandey, M. P., and Kim, C. S., *Chem. Eng. Technol.*, 2011, 34, 29-41.

[3] Ghodake, G. S., Shinde, S. K., Kadam, A. A., Saratale, R. G., Saratale, G. D., Kumar, M., Palem, R. R., AL-Shwaiman, H. A., Elgorban, A. M., Syed, A., and Kim, D. Y., *J. Clean. Prod.*, 2021, 297, 126645.

[4] Zakzeski, J., Bruijnincx, P. C., Jongerius, A. L., and Weckhuysen, B. M., *Chem. Rev.,* 2010, 110, 3552-3599.

[5] Yang, H. M., Apparia, S., Kudo, S., Hayash, J., and Norinaga, K., *Ind. Eng. Chem. Res.*, 2015, 54, 6855-6864.

[6] Yu, J., Wang, D., Sun, L., *Fuel*, 2021, 290, 120078.

[7] Zakzeski, J., Bruijnincx, P. C., Jongerius, A. L., and Weckhuysen, B. M., *Chem. Rev.*, 2010, 110: 3552-3599.

[8] Zhang, L., Choi, C., Machida, H., and Norinaga, K., *J. Anal. Appl. Pyrol.*, 2021, 156, 105096.

[9] Jiang, G. Z., Nowakowski, D. J., and Bridgwater, A. V., *Energ. Fuel*, 2010, 24, 4470 - 4475.

[10] Zhou, S., Garcia-Perez, M., Pecha, B., McDonald, A. G., and Kersten, S. R. A., Westerhof, R. J. M., Energ. *Fuel*, 2013, 27, 1428-1438.

[11] Mansouri, N.E.E., and Salvadó, J., *Ind. Crop. Prod.* 2006, 24, 8-16.

[12] Azadi, P. O., Inderwildi, R., Farnood, R., and King, D. A., *Renew. Sust. Energ. Rev.*, 2013, 21, 506-523.

[13] Victoria, B., Custodis, F., Hemberger, P., Ma, Z., and Bokhoven, J. A., *J. Phys. Chem. B*, 2014, 118, 852-8531.

[14] Chu, S., Subrahmanyam, A. V., and Huber, G. W., *Green Chem.*, 2013, 15, 125-136.

[15] Jarvis, M. W., Daily, J. W., Carstensen, H. H., Dean, A. M., Sharma, S., Dayton, D. C., Robichaud, J. D., and Nimlos, R. M., *J. Phys. Chem. A*, 2011, 115, 428-438.

[16] Choi, S. Y., Singh, R., Zhang, J., Balasubramanian, G., Sturgeon, R. M., Katahira, R., Chupka, G., Beckhamc, T. G., and Shanks, H. B., *Green Chem.*, 2016, 18, 1762-1773.

[17] Huang, J., He, C., Liu, C., Tong, H., Wu, L., and Wu, S., *Comput. Theor. Chem.*, 2015, 1054, 80-87.

[18] Scheer, A. M., Mukarakate, C., Robichaud, D. J., Nimlos, M. R., Carstensen, H. H., and Ellison, G. B., *J. Chem. Phys. A,* 2012, 136, 044309.

[19] Yang, H. M., Furutani, Y., Kudo, S., Hayash, J., and Norinaga, K., *J. Anal. Appl. Pyrol.*, 2016, 120, 321-329.

[20] Scheer, A. M., Mukarakate, C., Robichaud, D. J., Ellison, G. B., and Nimlos, M. R., *J. Phys. Chem. A*, 2010, 114, 9043–9056.

[21] Scheer, A. M., Mukarakate, C., Robichaud, D. J., Nimlos, M. R., and Ellison, G. B., *J. Phys. Chem. A*, 2011, 115, 13381-13389.

[22] Liu, C., Zhang, Y. Y., and Huang, X. L., *Fuel Process. Technol.*, 2014, 123, 159-165.

[23] Ledesma, E. B., Hoang, J. N., Nguyen, Q., Hernandez, V., Nguyen, M. P., Batamo, S., and Fortune, C. K., *Energ. Fuel*, 2013, 27, 6839-6846.

[24] Shin, E. J., Nimlos, M. R., Evans, R. J., *Fuel*, 2001, 80, 1689-1696.

[25] Huang, J. B., Liu, C., Ren, L. R., Tong, H., Li, W. M., and Wu, D., *J. Fuel Chemistry Technolog.*, 2013, 41, 657-666.

[26] Asmadi, M., Kawamoto, H., and Saka, S., *J. Anal. Appl. Pyrol.*, 2011, 92, 88-98.